Influence of cerium oxide nanoparticles on thermal conductivity of antifreeze

Preparation and stability of nanofluid using surfactant

Ali Taghizadeh[1] · Mohsen Taghizadeh[1] · Mohammad Azimi[1] · Ali Sulaiman Alsagri[2] · Abdulrahman A. Alrobaian[3] · Masoud Afrand[4,5]

Abstract

The objective of this work was to examine the thermal conductivity of a stable nano-antifreeze containing cetyltrimethylammonium bromide coated cerium (IV) oxide nanoparticles (CeO_2 NPs). The considered base fluid is a mixture of 50:50 ethylene glycol (EG) and deionized water. The morphology and structure of the samples are characterized with X-ray diffraction, field emission scanning electron microscopy, energy-dispersive X-ray analysis, and Fourier-transform infrared spectroscopy. The experiments are done in the volume concentration range of 0.1–0.9%, CNT volume concentration range of 0.015–0.135% and the temperature range of 20–50 °C. The thermal conductivity (TC) of the prepared nanofluid samples was measured using a KD2-Pro thermal properties analyzer. The outcomes showed that boosting the temperature and the solid volume concentration causes an increase in the thermal conductivity ratio of the CeO_2/EG–water nanofluid. The findings also indicated that the TC of CeO_2/EG–water nanofluid augments up to 36.13% at volume concentration of 0.135% and 50 °C. Furthermore, it was depicted that the use of CeO_2 NPs lead to a higher TC compared to other NPs in the same base fluid. Finally, a new correlation was proposed for predicting the TC and thermal conductivity enhancement of CeO_2/EG–water in terms of nanoparticle concentration and temperature.

Keywords Cerium (IV) oxide · New nano-antifreeze · Thermal conductivity · Stability · Surfactant

Abbreviations

CTAB	Cetyltrimethylammonium bromide
CMC	Critical micelle concentration
NP	Nanoparticle
TC	Thermal conductivity ($W\ m^{-1}\ K^{-1}$)
EG	Ethylene glycol
TCE	Thermal conductivity enhancement
TCR	Thermal conductivity ratio
FESEM	Field emission scanning electron microscopy
FTIR	Fourier transform infrared spectroscopy
XRD	X-ray diffraction
EDAX	Energy-dispersive X-ray analysis

✉ Masoud Afrand
masoud.afrand@tdtu.edu.vn

Ali Sulaiman Alsagri
a.alsagri@qu.edu.sa

Abdulrahman A. Alrobaian
Alrobaian@qu.edu.sa

[1] Department of Mechanical Engineering, Najafabad Branch, Islamic Azad University, Najafabad, Iran

[2] Mechanical Engineering Department, Unayzah College of Engineering, Qassim University, Qassim 51911, Saudi Arabia

[3] Mechanical Engineering Department, College of Engineering, Qassim University, Qassim 51452, Saudi Arabia

[4] Laboratory of Magnetism and Magnetic Materials, Advanced Institute of Materials Science, Ton Duc Thang University, Ho Chi Minh City, Vietnam

[5] Faculty of Applied Sciences, Ton Duc Thang University, Ho Chi Minh City, Vietnam

List of symbols

K Dimensionless shape factor
D Average crystal size (Å)
B The line broadening at half the maximum intensity (radian)
Λ X-ray wavelength
Θ The Bragg angle (°)

Introduction

In recent years, various studies have been done to evaluate the thermophysical properties of water to develop its application in various industries. One of the most convenient methods of reduction of water freezing point is the addition of EG. The mixture of EG and water is known as an efficient antifreeze in cold regions. In fact, this mixture has a lower TC in comparison with the pure water.

Nanofluids are a new class of heat transfer fluid incorporating a small quantity of nanosized particles that are uniformly and stably suspended in common liquids such as water and engine oil [1]. Nanofluids have many applications in various fields such as chemical and environmental engineering [2–5]. Previous studies have revealed that the TC of nanofluids is higher than that of the base fluids [6]. In addition, it has been reported that the TC of nanofluids is highly sensitive to several factors such as size, shape, aspect ratio, NP concentration, temperature, base fluid, pH, and surfactant type and also many studies have focused on thermal convection improvement as desired change and also rheological changes to check viscosity increase as unwanted phenomena after adding nanoparticles to base fluids [6–19]. The presence of dispersed NPs within the range of 1–100 nm in nanofluids can significantly enhance the TC and the viscosity of base fluids [20]. Hence, nanofluids have been noted by many scholars and scientists because of their advantageous for several modern uses, and researchers have believed that they are the modern heat transfer fluids [21–23].

Several researchers have focused on the TCE of nanofluids with base fluids like water, EG, and EG–water mixture. Syam Sundar et al. [24] studied the thermophysical aspects of Fe_3O_4/EG–water nanofluid at ratios 60:40, 40:60, and 20:80 and reported the highest TCE of 2.94% which was for the 60:40 mixture. Vajjha and Das [25] investigated the TCE of mixture of 60:40 EG–water containing CuO and Al_2O_3 NPs. Reddy and Rao [26] reported the TC of TiO_2/EG–water nanofluid samples in the temperature range of 30–70 °C and the volume concentration range of 0.2–1.0%. They noticed that the TC of this type of nanofluid could increase up to about 7%. Suganthi et al. [27] examined the TC of ZnO/EG–water (50:50) nanofluid and reported the maximum TCE of 17.26% for the nanofluid with volume concentration of 2%. Teng and Yu [28] showed that the TCE of nanofluid Al_2O_3/EG–water (45:55) nanofluid with volume concentration of 3% is about 11.6%. Hemmat Esfe et al. [29–31] depicted that the TCE of 40:60 EG–water nanofluid containing CuO, MgO and Cu/TiO_2 NPs is 36.97%, 35%, and 44%, respectively. Afrand et al. [32] examined the TC of Fe_3O_4/water nanofluid in the temperature range of 20–55 °C and volume concentration range of 0.1–3%. In an experimental investigation, Sundar et al. [33] studied the TC of Fe_2O_4/EG–water nanofluid and found that the maximum TCE belongs to the 20:80 EG–water mixture with NP concentration of 2%. They also reported that the TC augments by boosting both the NP concentration and temperature. Soltanimehr and Afrand [1] investigated the influence of operational parameters on the TC of MWCNT/EG–water nanofluid. The outcomes of their research showed that the maximum TCE of this nanofluid is about 34.7%. Keyvani et al. [34] studied the TCE of CeO_2/water nanofluid. The findings revealed that the highest TCE is about 22% which belonged to the nanofluid with NP concentration of 2.5% at 50 °C. Some was performed on thermal behavior of nanofluids with CeO_2 NPs and different base fluids [35–38].

Table 1 presents a brief summary of other researches work. In these works, water or ethylene glycol was used as the base fluid. According to the results of these studies, increasing NP concentration in water or ethylene glycol enhances the TC of the base fluid.

One of the main requirements of nanofluids is their long-term stability. The preparation method of a nanofluid is very important because of its direct impact on its thermophysical properties such as the TC. Literature survey shows that numerous inconsistencies exist in the available data regarding the nanofluids stability. Indeed, the key factor which affects the nanofluid stability is aggregation of NPs due to the existence of van der waals attractive forces. In fact, the instability of nanofluids is the main disadvantage for industrial applications [45–47]. Nanoparticles tend to aggregate since surface area and surface activity of these particles are high [48]. To achieve stable nanofluids, researchers use physical or chemical techniques such as the addition of surfactant, surface adjustment of the suspended particles or inducing a strong external force on the NP clusters. Among these techniques, the use of surfactant is one of the most efficient methods [49, 50]. Surfactants can be anionic, cationic, non-ionic and amphoteric [51]. Various scholars have used surfactants to make stable nanofluids. Leong et al. [52] studied the stability and TC of the carbon nanotube/EG–water nanofluid with/without a surfactant. Table 2 summarizes some of the examples of surfactants.

Table 1 TCE of various nanofluids

References	Particles	Size/nm	Base fluid	Concentration/%	Max Enhancement
Hemmat Esfe et al. [39]	$Mg(OH)_2$	20	EG	0.1–2	0.1–2
Afrand et al. [40]	Fe_3O_4	20–30	Water	0.1–3	0.1–3
Cho et al. [41]	Si	200	EG	10,000 mg/L	10,000 mg/L
Chen et al. [42]	CNT	10	Water	0.3–1	0.3–1
Glory et al. [43]	MWCNT	0.5	Water	0.24	0.24
Angayarkanni et al. [44]	TiO_2	13	Water	1–4	1–4

Table 2 Common surfactants used by researchers

Type of surfactant	Most used by researchers
Cationic	Distearyldimethylammonium chloride, benzalkonium chloride, cetrimonium chloride, cetyltrimethylammonium bromide (CTAB)
Anionic	Sodium dodecyl sulfate (SDS), Sodium dodecylbenzenesulphonate (SDBS)
Non-ionic	Polyvinyl pyrrolidone (PVP), Rokacet O7, Polyoxyethylene (10) nonyl phenyl ether, Tween X-100, oleic acid, Gum arabic (GA), Tween 80

Kim et al. [53] applied the SDS and CTAB for dispersing carbon nanotubes in water and the concentration of each surfactant was nearly 0.3 mass%. Li et al. [54] focused on spreading the performance of aqueous copper nanofluids. They investigated CTAB, SDBS, and Polyoxyethylene (10) nonyl phenyl ether (TX-10). Their work showed that the optimum concentration for TX-10, CATB, and SDBS is 0.43%, 0.05%, and 0.07%, respectively. Hemmat Esfe et al. [55] applied Cetyltrimethylammonium Bromide (CTAB) to warrant high stability and good dispersion of different nanofluids.

To have better insight, Table 3 shows the comparison of different surfactant and nanofluid combinations reported in the literature.

In this study, for the first time, the TC of cerium oxide/ethylene glycol–water (50:50) nanofluid has been evaluated. Stable nanofluid samples containing cerium oxide NPs in EG–water base fluid were prepared through a two-step method. The stability and the TC of prepared samples are examined in the temperature range of 20–50 °C and volume concentration range of 0.015–0.135%. Characterization of CeO_2 NPs was conducted using the XRD, FTIR, FESM/EDAX, and elemental mapping techniques. Cetyltrimethylammonium bromide (CTAB) was applied as surfactant to improve the stability of suspended NPs. Although it seems that adding surfactant is an efficient and economical approach to increase the nanofluids stability, the existence of surfactant can increase the thermal resistance and weakens the heat transfer performance of nanofluids. The dispersion behavior of nanofluid samples was examined to confirm nanofluid stability via different methods. The TC of the prepared samples was evaluated using the KD2-Pro at temperatures between 20 and 50 °C. In this research, a very small amount of CTAB was utilized to reduce the disadvantage of this method. Table 4 shows the review of the TCE of nanofluids with mixture of EG–water as base fluid. According to the results, the CeO_2/EG–water nanofluids with lower solid volume concentrations and at the same operating temperature range show better TCE in comparison with other nanofluids.

Experimental

Characterization of nanoparticles

The CeO_2 NPs (purity $\sim$ 99% and average diameter of 8–10 nm) were purchased from TECNAN company (Spain). Table 5 gives some physical properties of these NPs.

XRD Investigation

The crystal structure of the CeO_2 NPs was evaluated using a X'Pert Pro diffractometer (PANalytical, UK) equipped with a copper anode and a Cu Kα radiation source ($\lambda = 0.71$ Å). Figure 2 shows the XRD pattern of CeO_2 NPs. It is seen that the exact similarity of applied CeO_2 NP with the reference COD card (96-900-9009) which refer to the cerianite mineral. Miller indices, which related to the orientation of a surface or a crystal plane also, are given in Fig. 1.

The Sherrer formula [Eq. (1)] was applied for the estimation of the average crystallite size [61]. In this case, the average crystallite size of CeO_2 NPs is about 121 Å.

$$d = \frac{0.94\lambda}{B(2\theta)\cos\theta} \tag{1}$$

where d is the average crystalline size (nm), θ is the angle at maximum peak, λ stands for the wavelength of the incident X-ray and B denotes the full width at the half maximum intensity.

Table 3 Comparison of different surfactants and nanofluids

References	Particle	Surfactant	Base fluid
Song et al. [56]	Stainless steel	SDS, SDBS, CTAB	Water
Kim et al. [53]	CNT	CTAB	Water
Ghadimi and Metselaar [57]	TiO_2	SDS	Water

Table 4 TCE of nanofluids with mixture of EG–water as base fluid

References	Nanoparticle	EG/water ratio	Concentration/%	Max Enhancement
Keyvani et al. [34]	CeO_2	100:0	0.25–2.5	22
Hemmat Esfe et al. [30]	ZnO	40:60	0.1–3	~ 35
Ahmadi Nadooshan [58]	$TiO2/SiO_2$	30:70	0.125–4	20
Nabil et al. [59]	CuO	40:60	0.5–3	22.8
Hemmat Esfe et al. [29]	CuO	40:60	0.1–2	~ 33.8
Leong et al. [60]	Cu/TiO2	50:50	0.2–0.8	9.8
This study	CeO_2	50:50	0.015–0.135	36.1

Table 5 Some physical properties of CeO_2 NPs

| Properties	Values
Specific surface area (SSA)	85–170 $m^2\ g^{-1}$
Nanopowder (CeO_2) color	Light yellow
Density	7.22 $g\ cm^{-3}$
Average particle size (APS)	8–10 nm
Formula weight	172.12 $mol\ g^{-1}$
Melting point	2600 °C
Purity	99.721%

FESEM and EDAX examination

Field emission scanning electron microscopy (FESEM) was performed using ZEISS SIGMA 500 VP FESEM (ZEISS company, Germany), and the obtained results are presented in Fig. 2a. It is seen that the average diameter of NPs is on the order of 15 nm, which is in good agreement with the XRD analysis. As shown in Fig. 2b, the energy-dispersive X-ray analysis (EDAX) spectrum of CeO_2 demonstrates peaks of Ce and O. Energy-dispersive X-ray analysis (EDAX) and Mapping was measured by Oxford instrument, England.

To verify FESEM, the dynamic light scattering (DLS) analysis was done by ZENZS 3690 NANO SERIES, UK in two mass concentration of CeO_2 NPs. Figure 3 shows the particle distribution of CeO_2 in the base fluid. The findings revealed that the average particle size of CeO_2 NPs is about 8.392 nm and 7.780 nm at solid volume concentration of 0.035% and 0.135%.

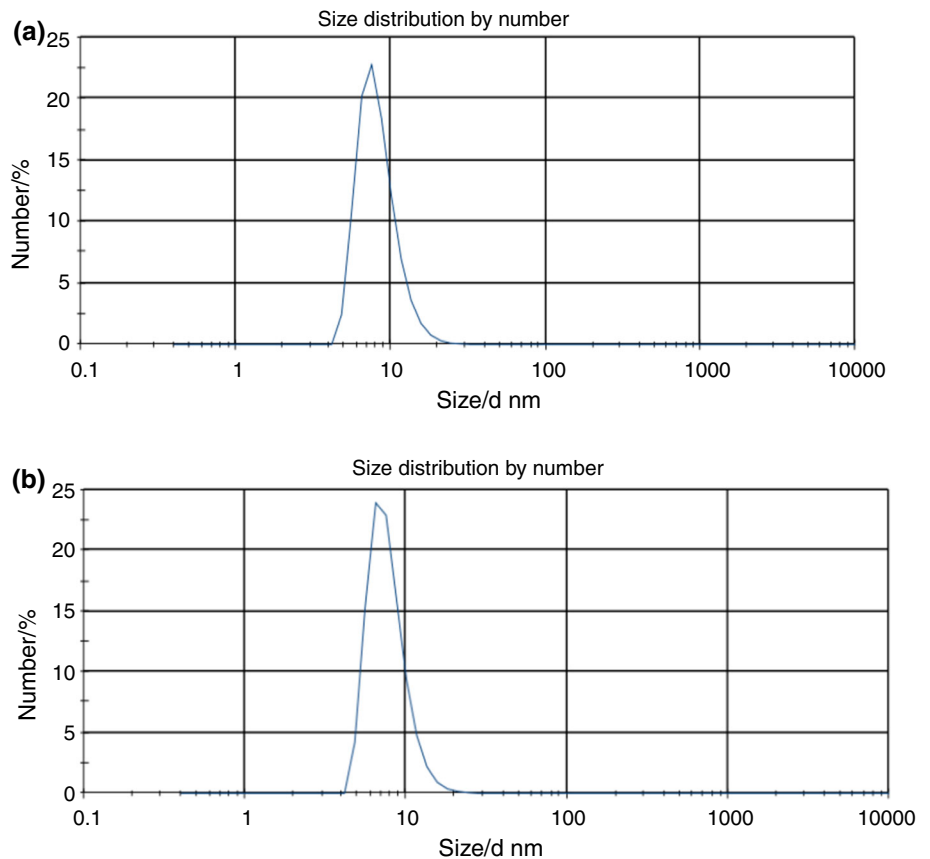## Dispersing and nanofluid preparation

To study the TC of nanofluids, the procedure of nanofluid preparation should be studied. According to the previous

Fig. 1 XRD pattern of CeO_2 NPs
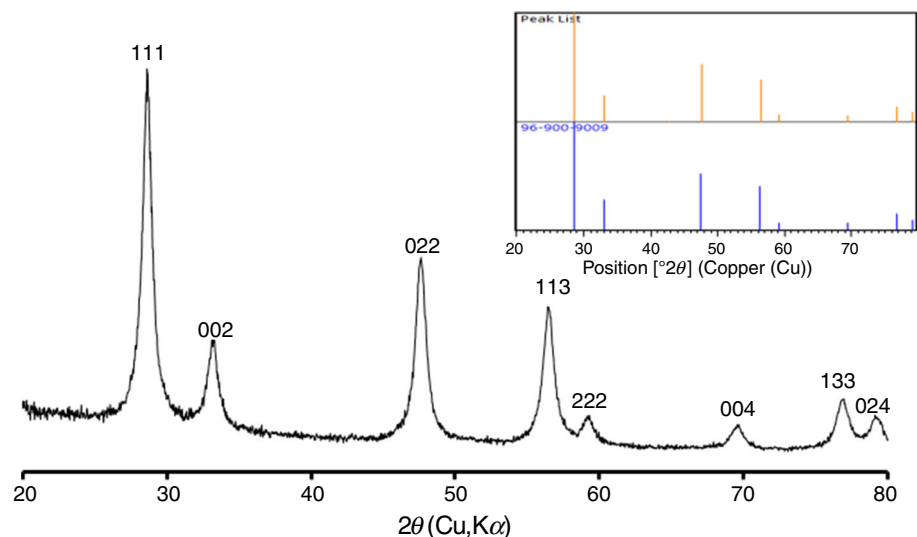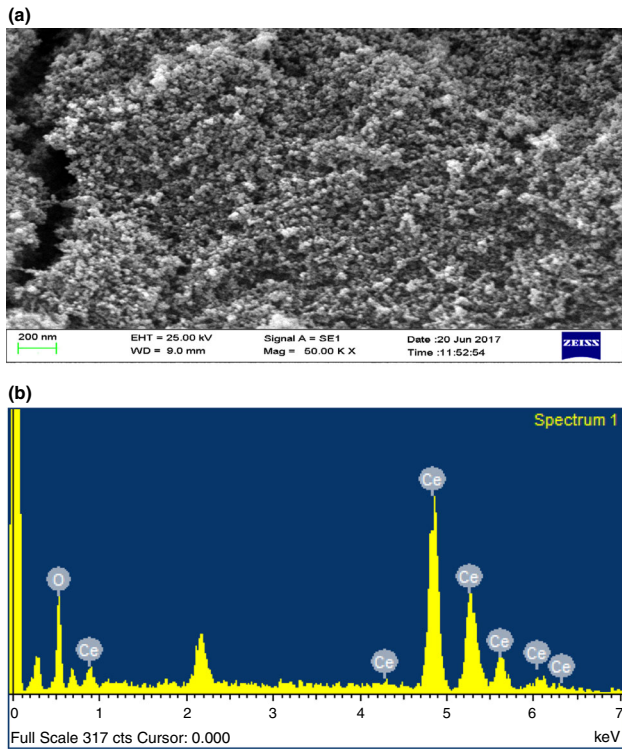
Fig. 2 FESEM image of CeO$_2$ NPs at ×50,000 magnification (**a**) and EDAX spectrum of CeO$_2$ NPs

studies, there are two methods for preparing a nanofluid including the single-step method and the two-step technique [26]. In this work, as the most common approach, the two-step technique is used to prepare the nanofluids. In this technique, NPs, nanofibers, nanotubes, or other nanomaterials are initially provided through chemical or physical procedures. In the next step, the nanosized powders are spread into a base fluid by using intensive magnetic force agitation, high-shear mixing, ultrasonic agitation, homogenizing, and ball milling. [18].

In this work, the considered base fluid was the 50:50 EG–water mixture. Table 6 gives some thermophysical properties of deionized water and EG. The certain amount of CTAB was added to the base fluid and sonicated for about 5 h by ultrasonic probe sonicator to get a 0.1% mass concentration solution. The required amount of CeO$_2$ is then calculated using Eq. (2). In fact, sonication of the nanofluid samples was done to gain better dispersion of NPs by removing the agglomerations of NPs.

$$\varphi = \left[\frac{\left(\frac{W}{\rho}\right)_{CeO_2}}{\left(\frac{W}{\rho}\right)_{CeO_2} + \left(\frac{W}{\rho}\right)_{basefluid}} \right] \times 100 \qquad (2)$$

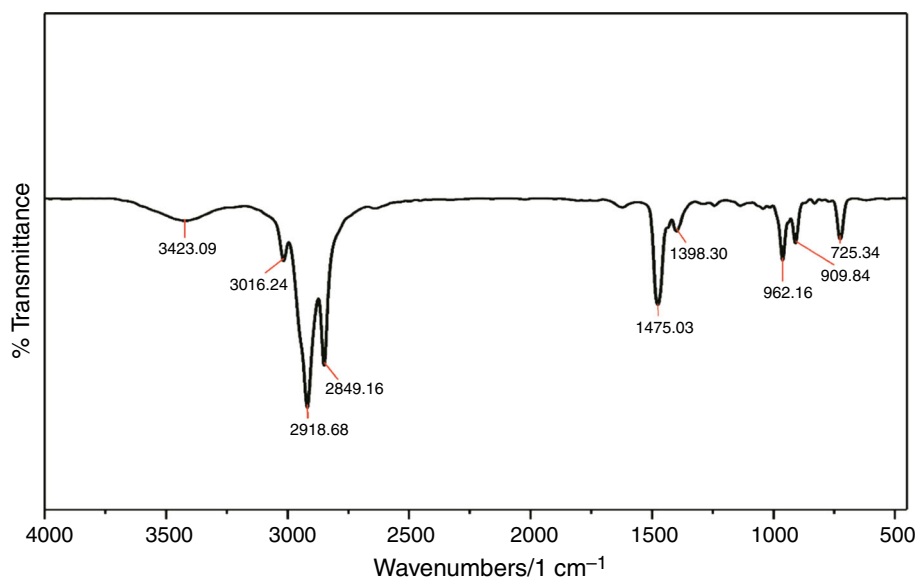where φ is the NP concentration, W is the mass and ρ is the density.

Fig. 3 Particle distribution of nanofluid **a** 0.035% and **b** 0.135%

Table 6 Some thermophysical properties of water and EG

Parameters	Water	EG
Purity	(Deionized water)	Extra pure 99.5%
Molar mass	18.015 g mol^{-1}	62.07 g mol^{-1}
Boiling point	100 °C	197.3 °C
Thermal conductivity	0.6 W m^{-1} K^{-1}	0.244 W m^{-1} K^{-1}
Density	998.21 kgm^{-3}	1113.2 kgm^{-3}

FTIR

The FTIR was applied to assess the formation of surfactant. In the FTIR spectrum, which is presented in Fig. 4, one peak at 3016 cm^{-1} is observed in the vas (N–CH$_3$) feature for the surfactants [62]. The absorption band at 2918 cm^{-1} was the characteristic peak for C–H stretch. Indeed, the vas (CH$_3$) feature located in a frequency lower than 2956 cm^{-1} indicates the crystalline structure and a crystalline phase occurs when the vsym (CH$_2$) frequency is lower than 2849 cm^{-1} [63–65]. The C–H stretching vibration- sym appeared at 2849 cm^{-1}. Two features of 1462 and 1472 cm^{-1} are related to the CH$_2$ scissoring region [66, 67]. CH$_2$ Wagging Region for the CTAB molecules occurs between 1300 and 1400 cm^{-1} [68]. Also, the peak at 1398 cm^{-1} is within the region of course. δ sym(N–CH$_3$) and ν(C–N) are also noticed at 1398 and 909 cm^{-1}, respectively, and they are in good agreement with the data in the literature [57]. Meanwhile, the peak appeared at 725 cm^{-1} was due to the C–H out-of-plane deformation vibration [69]. Therefore, the tail was also detected as a triplet peak at 0.90 mg L^{-1}.

Critical micelle concentration (CMC)

CMC is one of the main parameters for the evaluation of surfactants. In fact, CMC is the concentration in which surfactant mixture starts to form micelles in large scale. Electrical conductivity method is the simplest approach to define CMC. For this purpose, various concentrations of CTAB were prepared and the electrical conductivity of samples was measured. The results are depicted in Fig. 5. The sharp change in the slope indicates the CMC point of CTAB.

Stability investigation

The value of zeta potential is proportional to the stability of colloidal dispersions. Consequently, high-zeta-potential nanofluids, regardless of the type of surface charge, remain well stable, while low-zeta-potential nanofluids are unstable. According to the literature, the zeta potential values less than − 25 mV or more than + 25 mV can be considered as the stable fluids [70, 71]. For analyzing the agglomeration of NPs, the Zetasizer Nano Z (MALVERN ZENZS 3690 NANO SERIES, UK) was applied to study the zeta potential values of the samples. It was found that the zeta potential of the nanofluids with NP concentration of 0.015% and 0.135% are + 54.1 mV and + 59.9 mV, respectively (See Fig. 6). In the observation process, the prepared samples were examined in terms of the sedimentation of particles (Fig. 7), and it was found that the prepared nanofluids samples are stable for minimum 3 weeks.

Fig. 4 FTIR spectra of CTAB

Fig. 5 Electrical conductivity versus surfactant concentration
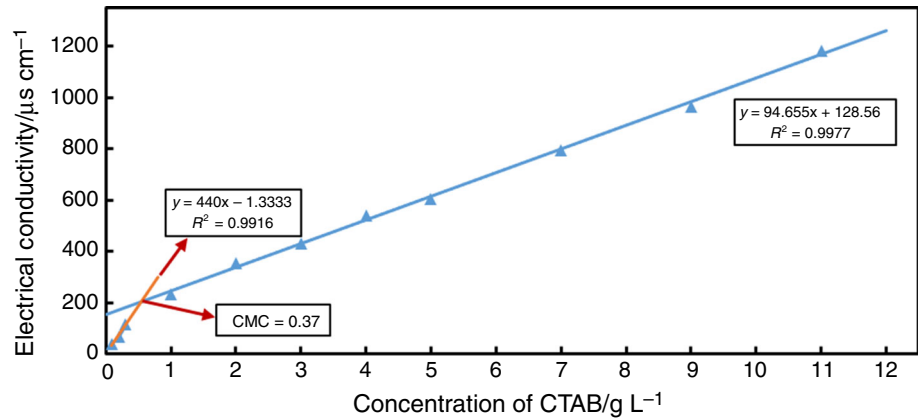
TC evaluation

To study the TC of CeO_2/EG–water nanofluid, five nanofluid samples with volume concentrations of 0.015%, 0.035%, 0.07%, 0.105%, and 0.135% are prepared using a cationic surfactant (CTAB) and the ultrasonic vibrator. To evaluate the TC of all nanofluids, a KD2-Pro thermal properties analyzer (Decagon devices, USA) was used. In this instrument, the well-known hot wire method is used. The samples were placed inside a glass vessel (15 mL) where the sensor was fixed vertically to reduce the error of measurement. The samples were maintained at several temperatures using a constant temperature water bath. After the temperature of the sample reached the required temperature, the sample was kept at that temperature for further 30 min to ensure temperature equilibrium before each measurement. The accuracy of the KD-2 device was tested by measuring the TC of 50:50 EG–water mixture and comparing the results with those of the ASHRAE [72] and Sundar et al. [33]. (See Fig. 8.) The obtained results showed that the device works properly and the error of the device is less than 3%.

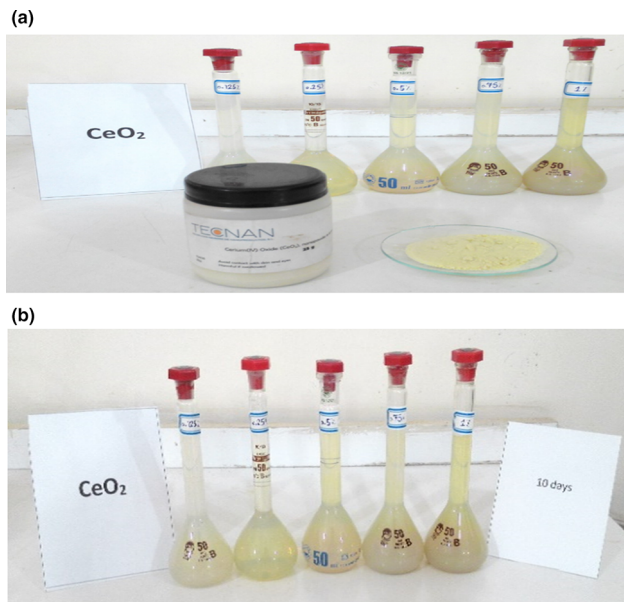**Fig. 6** Zeta potential for **a** 0.015% and **b** 0.135%

(a)

(b)
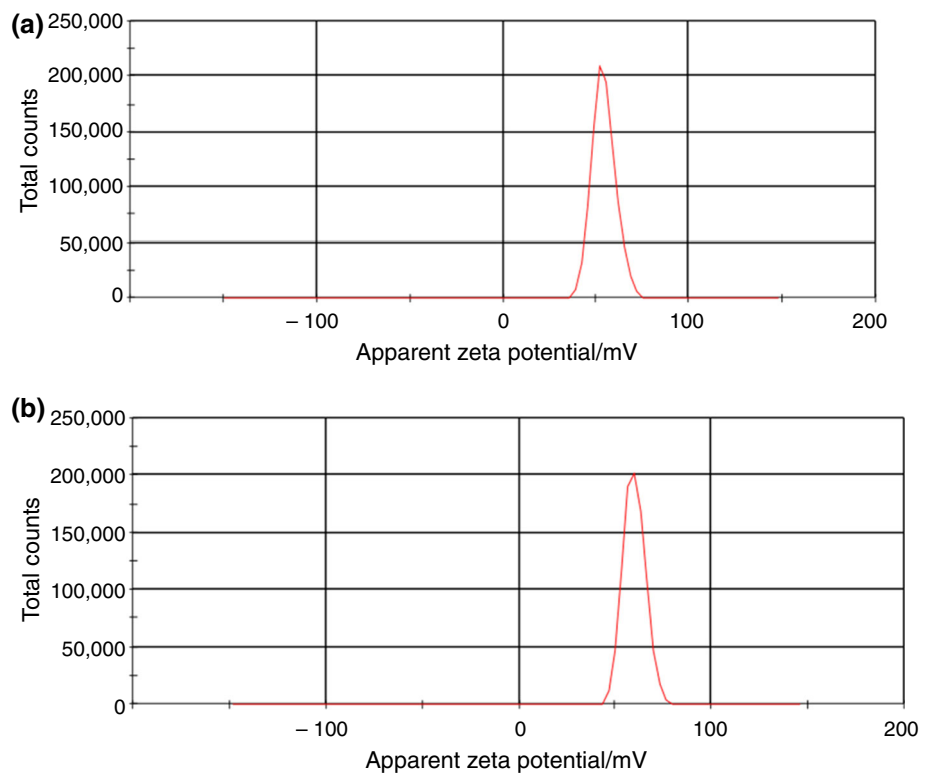
Fig. 7 Images of the dispersed nanofluids **a** after 2 days and **b** after 10 days
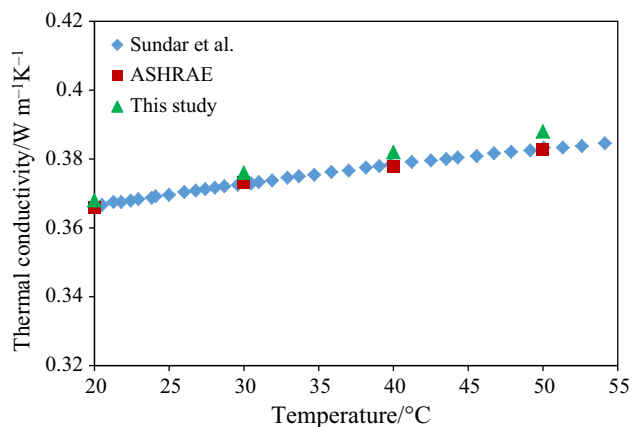

Fig. 8 Comparison of this experimental values and data available in the literature for EG–water 50:50% [29, 57]

Results and discussion

Figure 9 illustrates the variations of TC of CeO_2/EG–water nanofluid versus temperature for various NP concentrations. It is clear that the TC of nanofluid enhances by rising both the volume concentration and temperature. In addition, it is seen that the TCE is higher at higher temperatures.

Figure 10 demonstrates the TCE of nanofluid samples in various temperatures and volume concentrations. According to the findings, the highest TCE is 36.13% which belongs to the NP with volume concentration of 0.135% at 50 °C.
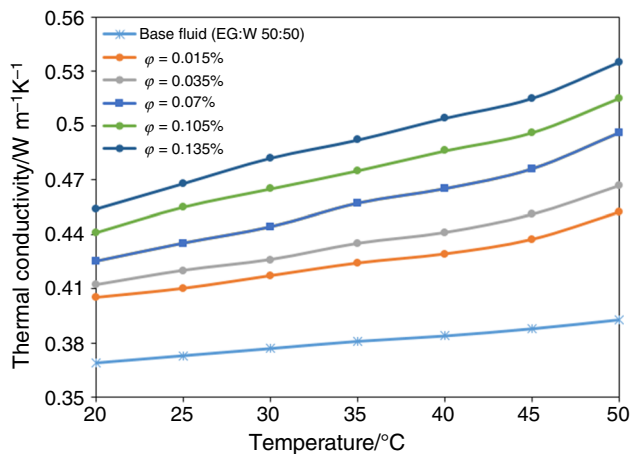

Fig. 9 TC of CeO_2/EG–water nanofluid versus temperature in different solid volume concentrations
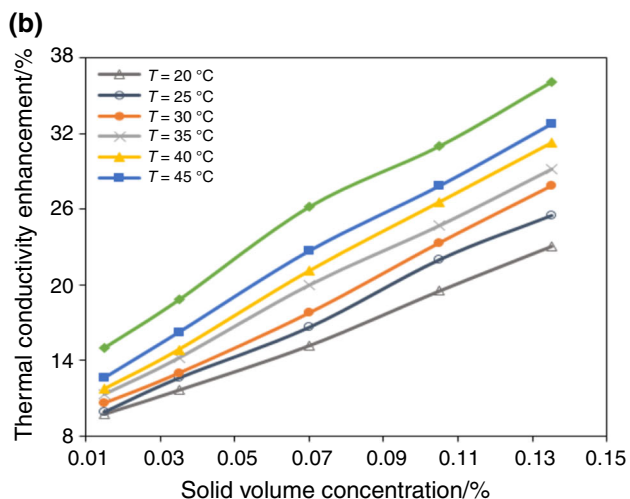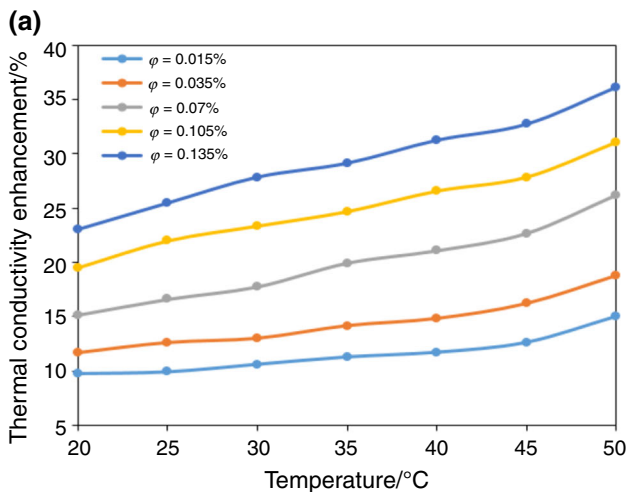
(a)

(b)

Fig. 10 TCE of the studied CeO_2/EG–water nanofluid samples

Figure 11 depicts the variations of the TCR (i.e., ratio of nanofluid TC and base fluid TC) versus NP concentration and temperature. The obtained results reveal that the TCR
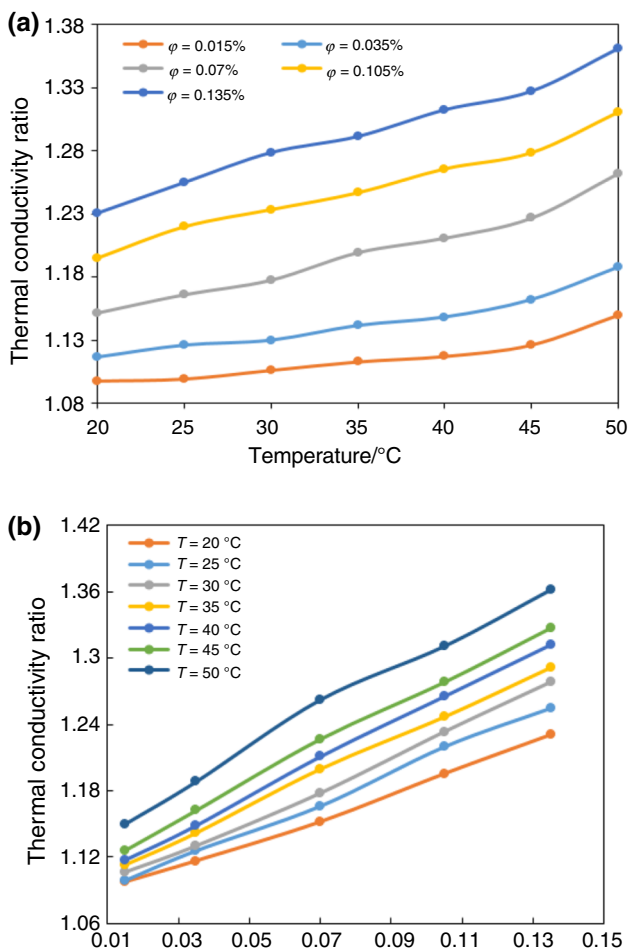
Fig. 11 TCR versus NP concentration and temperature

augments by boosting the volume concentration of NPs. Brownian motion and collisions between particles in high temperature are the main reasons for this observation. The results also demonstrate that the TCR intensifies with growing volume concentrations of NPs. Furthermore, the maximum TCR (i.e., 1.3613) is observed at 50 °C and volume concentration of 0.135%.

New correlation

According to the best knowledge of the authors, there is not an accurate and simple correlation for estimation of the TCE and TC of dispersed CeO_2 in 50:50 EG–water mixture. Equations (3) and (4) are proposed for the estimation of TCE and TC of CeO_2/EG–water nanofluid, respectively.

Thermal conductivity enhancement

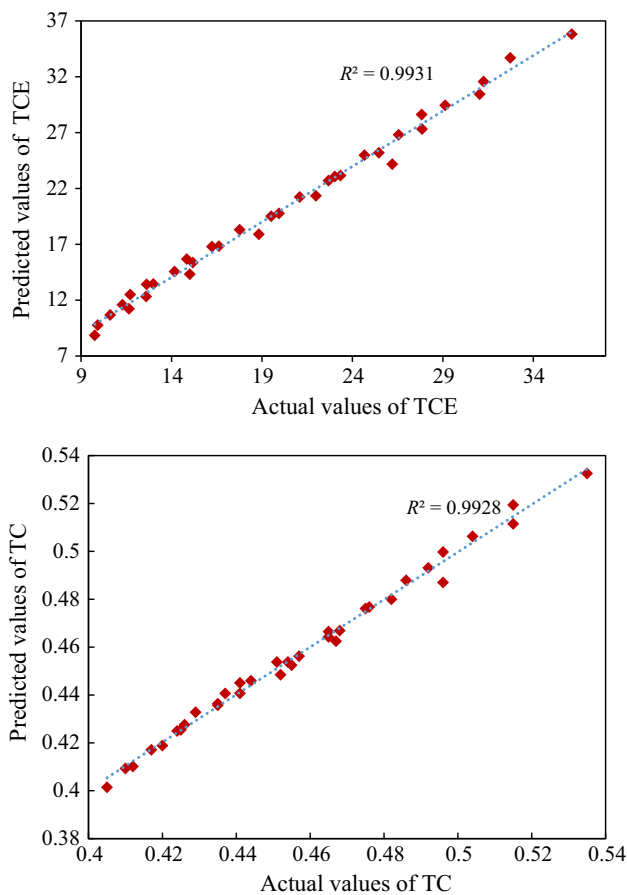$$= 0.152057T + 78.1569\varphi(\%) + 2.01932T.\varphi(\%) + 4.02839 \quad (3)$$

Fig. 12 Predicted versus actual values for TCE (up) and TC (down)

$$\begin{aligned} \text{Thermal conductivity} &= 0.00143474T + 0.25939\varphi(\%) \\ &\quad + 0.00882305T.\varphi(\%) \\ &\quad + 0.366217 \end{aligned}$$

$$(4)$$

These correlations are valid in the volume concentration range of 0.015–0.135% and temperature range of 20–50 °C. According to the coefficient of volume concentration in both equation, it can be concluded that the volume concentration of CeO_2 NPs has more influence on TCE and TC values as compared with the temperature. Figure 12 shows the predicted values of TCE and TC versus the actual values. The high value of R^2 indicates the accuracy of equations in the prediction of TCE and TC.

Conclusions

In this study, the stable CeO_2/EG–water nanofluid was successfully prepared and the stability of prepared samples was evaluated. The TC of the prepared nanofluid samples with 0.015%, 0.035%, 0.07%, 0.105%, and 0.135% solid volume concentrations were evaluated in the temperature

range of 20–50 °C. The findings confirmed that the TCR of the nanofluid could improve by boosting both the temperature and NP volume concentration. Additionally, it was found that the TC of CeO_2/EG–water nanofluid improves up to 36.13% when temperature and solid volume concentration are at the highest value. In addition, a new correlation was proposed for predicting the TC and TCE of nanofluid.

Future work

It is suggested that the rheological behavior of this nanofluid also be examined in order to be able to evaluate its efficiency using hydrothermal analysis of heat exchangers containing this nanofluid.

References

1. Soltanimehr M, Afrand M. Thermal conductivity enhancement of COOH-functionalized MWCNTs/ethylene glycol–water nanofluid for application in heating and cooling systems. Appl Therm Eng. 2016;105:716–23. https://doi.org/10.1016/j.applthermaleng.2016.03.089.
2. Al-Rashed AAAA, Shahsavar A, Entezari S, Moghimi MA, Adio SA, Nguyen TK. Numerical investigation of non-Newtonian water-CMC/CuO nanofluid flow in an offset strip-fin microchannel heat sink: thermal performance and thermodynamic considerations. Appl Therm Eng. 2019;155:247–58.
3. Al-Rashed AAAA, Shahsavar A, Rasooli O, Moghimi MA, Karimipour A, Tran MD. Numerical assessment into the hydrothermal and entropy generation characteristics of biological water–silver nano-fluid in a wavy walled microchannel heat sink. Int Commun Heat Mass Transf. 2019;104:118–26.
4. Esfe MH, Hajmohammad H, Toghraie D, Rostamian H, Mahian O, Wongwises S. Multi-objective optimization of nanofluid flow in double tube heat exchangers for applications in energy systems. Energy. 2017;137:160–71.
5. Shahsavar A, Rahimi Z, Salehipour H. Nanoparticle shape effects on thermal–hydraulic performance of boehmite alumina nanofluid in a horizontal double-pipe minichannel heat exchanger. Heat Mass Transf. 2019;55:1741–51. https://doi.org/10.1007/s00231-018-02558-x.
6. Esfe MH, Saedodin S, Biglari M, Rostamian H. Experimental investigation of thermal conductivity of CNTs-Al_2O_3/water: a statistical approach. Int Commun Heat Mass Transf. 2015;69:29–33.
7. Esfe MH, Saedodin S, Biglari M, Rostamian H. An experimental study on thermophysical properties and heat transfer characteristics of low volume concentrations of Ag-water nanofluid. Int Commun Heat Mass Transf. 2016;74:91–7.
8. Shahsavar A, Khanmohammadi S, Toghraie D, Salihepour H. Experimental investigation and develop ANNs by introducing the suitable architectures and training algorithms supported by sensitivity analysis: Measure thermal conductivity and viscosity for liquid paraffin based nanofluid containing Al_2O_3 nanoparticles. J Mol Liq. 2019;276:850–60.
9. Shahsavar A, Khanmohammadi S, Karimipour A, Goodarzi M. A novel comprehensive experimental study concerned synthesizes and prepare liquid paraffin–Fe_3O_4 mixture to develop models for both thermal conductivity and viscosity: a new approach of GMDH type of neural network. Int J Heat Mass Transf. 2019;131:432–41.
10. Mahian O, Kolsi L, Estellé P, Ahmadi G, Kleinstreuer C, Marshall JS, Siavashi M, Taylor RA, Niazmand H, Wongwises S, Hayat T, Kolanjiyil A, Kasaeian A, Pop I. Recent advances in modeling and simulation of nanofluid flows—part I: fundamental and theory. Phys Rep. 2018;1:1. https://doi.org/10.1016/j.physrep.2018.11.004.
11. Mahian O, Kolsi L, Amani M, Estellé P, Ahmadi G, Kleinstreuer C, Marshall JS, Taylor RA, Abu-Nada E, Rashidi S, Niazmand H, Wongwises S, Hayat T, Kasaeian A, Pop I. Recent advances in modeling and simulation of nanofluid flows—part II: applications. Phys Rep. 2018. https://doi.org/10.1016/J.PHYSREP.2018.11.003.
12. Hemmat Esfe MH, Rejvani M, Karimpour R, Arani AAA. Estimation of thermal conductivity of ethylene glycol-based nanofluid with hybrid suspensions of SWCNT–Al_2O_3 nanoparticles by correlation and ANN methods using experimental data. J Therm Anal Calorim. 2017;128(3):1359–71.
13. Hemmat Esfe MH, Hajmohammad MH. Thermal conductivity and viscosity optimization of nanodiamond-Co3O4/EG (40: 60) aqueous nanofluid using NSGA-II coupled with RSM. J Mol Liq. 2017;238:545–52.
14. Hemmat Esfe MH, Esfandeh S, Rejvani M. Modeling of thermal conductivity of MWCNT-SiO_2 (30: 70%)/EG hybrid nanofluid, sensitivity analyzing and cost performance for industrial applications. J Therm Anal Calorim. 2018;131(2):1437–47.
15. Hemmat Esfe MH, Esfandeh S, Amiri MK, Afrand M. A novel applicable experimental study on the thermal behavior of SWCNTs (60%)-MgO (40%)/EG hybrid nanofluid by focusing on the thermal conductivity. Powder Technol. 2019;342:998–1007.
16. Hemmat Esfe MH, Rostamian H, Sarlak MR, Rejvani M, Alirezaie A. Rheological behavior characteristics of TiO_2-MWCNT/10w40 hybrid nano-oil affected by temperature, concentration and shear rate: an experimental study and a neural network simulating. Phys E Low-dimen Syst Nanostruct. 2017;94:231–40.
17. Hemmat Esfe MH, Saedodin S, Rejvani M, Shahram J. Experimental investigation, model development and sensitivity analysis of rheological behavior of ZnO/10W40 nano-lubricants for automotive applications. Phys E Low-dimen Syst Nanostruct. 2017;90:194–203.
18. Hemmat Esfe MH, Hajmohammad H, Moradi R, Arani AAA. Multi-objective optimization of cost and thermal performance of double walled carbon nanotubes/water nanofluids by NSGA-II using response surface method. Appl Therm Eng. 2017;112:1648–57.
19. Hemmat Esfe MH, Arani AAA, Niroumand AH, Yan WM, Karimipour A. Mixed convection heat transfer from surface-mounted block heat sources in a horizontal channel with nanofluids. Int J Heat Mass Transf. 2015;89:783–91.
20. Shahsavar A, Salimpour MR, Saghafian M, Shafii MB. An experimental study on the effect of ultrasonication on thermal conductivity of ferrofluid loaded with carbon nanotubes. Thermochim Acta. 2015;617:102–10.
21. Alsarraf J, Bagherzadeh SA, Shahsavar A, Rostamzadeh M, Trinh PV, Tran MD. Rheological properties of SWCNT/EG mixture by a new developed optimization approach of LS-support vector regression according to empirical data. Phys A. 2019;525:912–20.
22. Liu WI, Alsarraf J, Shahsavar A, Rostamzadeh M, Afrand M, Nguyen TK. Impact of oscillating magnetic field on the thermal-conductivity of water–Fe_3O_4 and water–Fe_3O_4/CNT ferro-fluids: experimental study. J Magn Magn Mater. 2019;484:258–65.

23. Monfared M, Shahsavar A, Bahrebar MR. Second law analysis of turbulent convection flow of boehmite alumina nanofluid inside a double-pipe heat exchanger considering various shapes for nanoparticle. J Therm Anal Calorim. 2019;135:1521–32.

24. Syam Sundar L, Venkata Ramana E, Singh MK, De Sousa ACM. Viscosity of low volume concentrations of magnetic Fe_3O_4 nanoparticles dispersed in ethylene glycol and water mixture. Chem Phys Lett. 2012;554:236–42. https://doi.org/10.1016/j.cplett.2012.10.042.

25. Vajjha RS, Das DK. Experimental determination of thermal conductivity of three nanofluids and development of new correlations. Int J Heat Mass Transf. 2009;52:4675–82. https://doi.org/10.1016/j.ijheatmasstransfer.2009.06.027.

26. Reddy MCS, Rao VV. Experimental studies on thermal conductivity of blends of ethylene glycol–water-based TiO_2 nanofluids. Int Commun Heat Mass Transf. 2013;46:31–6. https://doi.org/10.1016/j.icheatmasstransfer.2013.05.009.

27. Suganthi KS, Leela Vinodhan V, Rajan KS. Heat transfer performance and transport properties of ZnO–ethylene glycol and ZnO–ethylene glycol–water nanofluid coolants. Appl Energy. 2014;135:548–59. https://doi.org/10.1016/j.apenergy.2014.09.023.

28. Teng TP, Yu CC. Heat dissipation performance of MWCNTs nano-coolant for vehicle. Exp Therm Fluid Sci. 2013;49:22–30. https://doi.org/10.1016/j.expthermflusci.2013.03.007.

29. Hemmat Esfe M, Saedodin S, Akbari M, Karimipour A, Afrand M, Wongwises S, Safaei MR, Dahari M. Experimental investigation and development of new correlations for thermal conductivity of CuO/EG–water nanofluid. Int Commun Heat Mass Transf. 2015;65:47–51. https://doi.org/10.1016/j.icheatmasstransfer.2015.04.006.

30. Hemmat Esfe M, Afrand M, Karimipour A, Yan W-M, Sina N. An experimental study on thermal conductivity of MgO nanoparticles suspended in a binary mixture of water and ethylene glycol. Int Commun Heat Mass Transf. 2015;67:173–5. https://doi.org/10.1016/J.ICHEATMASSTRANSFER.2015.07.009.

31. Hemmat Esfe M, Wongwises S, Naderi A, Asadi A, Safaei MR, Rostamian H, Dahari M, Karimipour A. Thermal conductivity of Cu/TiO_2–water/EG hybrid nanofluid: experimental data and modeling using artificial neural network and correlation. Int Commun Heat Mass Transf. 2015;66:100–4. https://doi.org/10.1016/j.icheatmasstransfer.2015.05.014.

32. Afrand M, Toghraie D, Sina N. Experimental study on thermal conductivity of water-based Fe_3O_4 nanofluid: development of a new correlation and modeled by artificial neural network. Int Commun Heat Mass Transf. 2016;75:262–9. https://doi.org/10.1016/j.icheatmasstransfer.2016.04.023.

33. Sundar LS, Singh MK, Sousa ACM. Thermal conductivity of ethylene glycol and water mixture based Fe_3O_4 nanofluid. Int Commun Heat Mass Transf. 2013;49:17–24. https://doi.org/10.1016/j.icheatmasstransfer.2013.08.026.

34. Keyvani M, Afrand M, Toghraie D, Reiszadeh M. An experimental study on the thermal conductivity of cerium oxide/ethylene glycol nanofluid: developing a new correlation. J Mol Liq. 2018;266:211–7. https://doi.org/10.1016/J.MOLLIQ.2018.06.010.

35. Sharafeldin MA, Gróf G. Evacuated tube solar collector performance using CeO_2/water nanofluid. J Clean Prod. 2018;185:347–56. https://doi.org/10.1016/j.jclepro.2018.03.054.

36. Sharafeldin MA, Gróf G. Experimental investigation of flat plate solar collector using CeO_2–water nanofluid. Energy Convers Manag. 2018;155:32–41. https://doi.org/10.1016/j.enconman.2017.10.070.

37. Akhgar A, Toghraie D. An experimental study on the stability and thermal conductivity of water-ethylene glycol/TiO_2–

MWCNTs hybrid nanofluid: developing a new correlation. Powder Technol. 2018;338:806–18. https://doi.org/10.1016/j.powtec.2018.07.086.

38. Kwon YH, Kim D, Li CG, Lee JK, Hong DS, Lee JG, Lee SH, Cho YH, Kim SH. Heat transfer and pressure drop characteristics of nanofluids in a plate heat exchanger. J Nanosci Nanotechnol. 2011;11:5769–74. https://doi.org/10.1166/jnn.2011.4399.

39. Hemmat Esfe M, Afrand M, Wongwises S, Naderi A, Asadi A, Rostami S, Akbari M. Applications of feedforward multilayer perceptron artificial neural networks and empirical correlation for prediction of thermal conductivity of $Mg(OH)_2$–EG using experimental data. Int Commun Heat Mass Transf. 2015;67:46–50. https://doi.org/10.1016/j.icheatmasstransfer.2015.06.015.

40. Afrand M, Toghraie D, Ruhani B. Effects of temperature and nanoparticles concentration on rheological behavior of Fe_3O_4–Ag/EG hybrid nanofluid: an experimental study. Exp Therm Fluid Sci. 2016;77:38–44. https://doi.org/10.1016/j.expthermflusci.2016.04.007.

41. Cho T, Baek I, Lee J, Park S. Preparation of nanofluids containing suspended silver particles for enhancing fluid thermal conductivity of fluids. J Ind Eng Chem. 2005;11:400–6.

42. Chen L, Xie H, Li Y, Yu W. Nanofluids containing carbon nanotubes treated by mechanochemical reaction. Thermochim Acta. 2008;477:21–4. https://doi.org/10.1016/j.tca.2008.08.001.

43. Glory J, Bonetti M, Helezen M, Mayne-L'Hermite M, Reynaud C. Thermal and electrical conductivities of water-based nanofluids prepared with long multiwalled carbon nanotubes. J Appl Phys. 2008;103:094309. https://doi.org/10.1063/1.2908229.

44. Angayarkanni SA, Philip J. Effect of nanoparticles aggregation on thermal and electrical conductivities of nanofluids. J Nanofluids. 2014;3:17–25. https://doi.org/10.1166/jon.2014.1083.

45. Shahsavar A, Salimpour MR, Saghafian M, Shafii MB. Experimental investigation on laminar forced convective heat transfer of ferrofluid loaded with carbon nanotubes under constant and alternating magnetic field. Exp Therm Fluid Sci. 2016;76:1–11.

46. Shahsavar A, Salimpour MR, Saghafian M, Shafii MB. Effect of magnetic field on thermal conductivity and viscosity of a magnetic nanofluid loaded with carbon nanotubes. J Mech Sci Technol. 2016;30:809–15.

47. Shahsavar A, Salimpour MR, Saghafian M, Shafii MB. Effect of temperature and concentration on thermal conductivity and viscosity of ferrofluid loaded with carbon nanotubes. Heat Mass Transf. 2016;52:2293–301.

48. Yu W, Xie H. A review on nanofluids: preparation, stability mechanisms, and applications. J Nanomater. 2012;2012:1–17. https://doi.org/10.1155/2012/435873.

49. Sidik NAC, Mohammed HA, Alawi OA, Samion S. A review on preparation methods and challenges of nanofluids. Int Commun Heat Mass Transf. 2014;54:115–25. https://doi.org/10.1016/j.icheatmasstransfer.2014.03.002.

50. Hwang Y, Park HS, Lee JK, Jung WH. Thermal conductivity and lubrication characteristics of nanofluids. Curr Appl Phys. 2006;6:e67–71. https://doi.org/10.1016/j.cap.2006.01.014.

51. Babita SK, Sharma SM. Gupta, Preparation and evaluation of stable nanofluids for heat transfer application: a review. Exp Therm Fluid Sci. 2016;79:202–12. https://doi.org/10.1016/j.expthermflusci.2016.06.029.

52. Leong K, Mohd Nurfadhillah H, Mohd S, Amer N. The effect of surfactant on stability and thermal conductivity of carbon nanotube based nanofluids. Therm Sci. 2016;20:429–36. https://doi.org/10.2298/TSCI130914078L.

53. Kim HS, Park WI, Kang M, Jin HJ. Multiple light scattering measurement and stability analysis. J Phys Chem Solids. 2008;69:1209–12. https://doi.org/10.1016/j.jpcs.2007.10.062.

54. Li X, Zhu D, Wang X. Evaluation on dispersion behavior of the aqueous copper nano-suspensions. J Colloid Interface Sci. 2007;310:456–63. https://doi.org/10.1016/j.jcis.2007.02.067.

55. Hemmat Esfe M, Abbasian Arani AA, Rezaie M, Yan W-M, Karimipour A. Experimental determination of thermal conductivity and dynamic viscosity of Ag–MgO/water hybrid nanofluid. Int Commun Heat Mass Transf. 2015;66:189–95. https://doi.org/10.1016/j.icheatmasstransfer.2015.06.003.

56. Song YY, Bhadeshia HKDH, Suh D-W. Stability of stainless-steel nanoparticle and water mixtures. Powder Technol. 2015;272:34–44. https://doi.org/10.1016/j.powtec.2014.11.026.

57. Ghadimi A, Metselaar IH. The influence of surfactant and ultrasonic processing on improvement of stability, thermal conductivity and viscosity of titania nanofluid. Exp Therm Fluid Sci. 2013;51:1–9. https://doi.org/10.1016/j.expthermflusci.2013.06.001.

58. Ahmadi Nadooshan A. An experimental correlation approach for predicting thermal conductivity of water–EG based nanofluids of zinc oxide. Phys E Low Dimens Syst Nanostruct. 2017;87:15–9. https://doi.org/10.1016/j.physe.2016.11.004.

59. Nabil MF, Azmi WH, Abdul Hamid K, Mamat R, Hagos FY. An experimental study on the thermal conductivity and dynamic viscosity of TiO_2–SiO_2 nanofluids in water: ethylene glycol mixture. Int Commun Heat Mass Transf. 2017;86:181–9. https://doi.org/10.1016/j.icheatmasstransfer.2017.05.024.

60. Leong KY, Razali I, Ahmad KZK, Ong HC, Ghazali MJ, Abdul Rahman MR. Thermal conductivity of an ethylene glycol/water-based nanofluid with copper–titanium dioxide nanoparticles: an experimental approach. Int Commun Heat Mass Transf. 2018;90:23–8. https://doi.org/10.1016/j.icheatmasstransfer.2017.10.005.

61. Hemmat Esfe M, Yan W-M, Afrand M, Sarraf M, Toghraie D, Dahari M. Estimation of thermal conductivity of Al_2O_3/water (40%)–ethylene glycol (60%) by artificial neural network and correlation using experimental data. Int Commun Heat Mass Transf. 2016;74:125–8. https://doi.org/10.1016/j.icheatmasstransfer.2016.02.002.

62. Xue W, He H, Zhu J, Yuan P. FTIR investigation of CTAB-Al-montmorillonite complexes. Spectrochim Acta Part A Mol Biomol Spectrosc. 2007;67:1030–6. https://doi.org/10.1016/j.saa.2006.09.024.

63. Sperline RP. Infrared spectroscopic study of the crystalline phases of sodium dodecyl sulfate. Langmuir. 1997;13:3715–26. https://doi.org/10.1021/la9702087.

64. Kawai T, Umemura J, Takenaka T, Kodama M, Seki S. Fourier transform infrared study on the phase transitions of an octadecyltrimethylammonium chloride–water system. J Colloid Interface Sci. 1985;103:56–61. https://doi.org/10.1016/0021-9797(85)90076-1.

65. Padalkar KV, Gaikar VG, Aswal VK. Characterization of mixed micelles of sodium cumene sulfonate with sodium dodecyl sulfate and cetyl trimethylammonium bromide by SANS, FTIR spectroscopy and NMR spectroscopy. J Mol Liq. 2009;144:40–9. https://doi.org/10.1016/j.molliq.2008.09.004.

66. Weers JG, Scheuing DR. Structure/performance relationships in monoalkyl/dialkyl cationic surfactant mixtures. J Colloid Interface Sci. 1991;145:563–80. https://doi.org/10.1016/0021-9797(91)90386-M.

67. Vaia RA, Teukolsky RK, Giannelis EP. Interlayer structure and molecular environment of alkylammonium layered silicates. Chem Mater. 1994;6:1017–22. https://doi.org/10.1021/cm00043a025.

68. Snyder RG. Vibrational study of the chain conformation of the liquid n-paraffins and molten polyethylene. J Chem Phys. 1967;47:1316–60. https://doi.org/10.1063/1.1712087.

69. Mahmoodi NM, Taghizadeh M, Taghizadeh A. Mesoporous activated carbons of low-cost agricultural bio-wastes with high adsorption capacity: preparation and artificial neural network modeling of dye removal from single and multicomponent (binary and ternary) systems. J Mol Liq. 2018;1:1. https://doi.org/10.1016/J.MOLLIQ.2018.07.108.

70. Ahammed N, Asirvatham LG, Titus J, Bose JR, Wongwises S. Measurement of thermal conductivity of graphene–water nanofluid at below and above ambient temperatures. Int Commun Heat Mass Transf. 2016;70:66–74. https://doi.org/10.1016/j.icheatmasstransfer.2015.11.002.

71. Sundar LS, Farooky MH, Sarada SN, Singh MK. Experimental thermal conductivity of ethylene glycol and water mixture based low volume concentration of Al_2O_3 and CuO nanofluids. Int Commun Heat Mass Transf. 2013;41:41–6. https://doi.org/10.1016/j.icheatmasstransfer.2012.11.004.

72. ASHRAE (American Society of Heating Refrigerating and Air-Conditioning Engineers). 2009 Ashrae handbook: fundamentals, I-P Edition. ASHRAE J. (2009). https://doi.org/10.1039/c1cs15219j.